Original Article

STK405759 targets microtubules, modulates STAT1, and enhances ruxolitinib efficacy in myeloproliferative neoplasms

Gabriela Rozic¹, Yaara Makaros², Irit Shapira-Netanelov¹, Tatiana Kardash¹, Yael Maizels¹, Igor Koman¹, Merav Leiba^{3,4*}, Adrian Duek^{3,4*}

¹Department of Molecular Biology, Institute for Personalized and Translational Medicine, Ariel University, Ariel, Israel; ²The Mina and Everard Goodman Faculty of Life Sciences, Bar-Ilan University, Ramat-Gan, Israel; ³Division of Hematology, Assuta Ashdod University Hospital, Ashdod, Israel; ⁴Faculty of Health Science, Ben-Gurion University of The Negev, Beer-Sheva, Israel. *Equal contributors.

Received August 27, 2025; Accepted October 25, 2025; Epub November 15, 2025; Published November 30, 2025

Abstract: Myeloproliferative neoplasms are clonal hematopoietic disorders characterized by excessive mature blood cells production, dysregulated JAK-STAT signaling, and increased angiogenesis. Current therapies, such as ruxolitinib, improve symptoms but lack disease-modifying effects. This study aimed to evaluate the cytotoxic and mechanistic effects of STK405759, a fully synthetic microtubule targeting agent in myeloproliferative neoplasms models. Three representative myeloproliferative neoplasms cell lines (HEL, SET-2, MEG-01) were treated with STK405759 as a single agent or in combination with ruxolitinib. Cytotoxicity was evaluated by XTT assays, apoptosis via Annexin V/propidium iodide staining, and cell cycle distribution by flow cytometry. Microtubule dynamics were examined by immunoblotting and immunofluorescence. Apoptosis-related proteins, cytokine secretion and JAK-STAT pathway activation were analyzed using antibody arrays, STK405759 showed potent cytotoxicity in JAK2 V617F-positive HEL and SET-2 cells and BCR-ABL1-positive MEG-01 cells. Combination with ruxolitinib yielded synergistic effects in HEL and SET-2 cells. Mechanistically, STK405759 disrupted microtubule organization, reduced α- and β-tubulin polymerization and acetylated α-tubulin, leading to G2/M arrest and apoptosis. In SET-2 cells, STK405759 significantly increased STAT1 phosphorylation while causing its retention in the cytoplasm. Treatment also decreased VEGF secretion in both monocultures and HS-5 stromal co-cultures and induced IL-1β in co-cultures. These findings demonstrate that STK405759 exerts potent cytotoxic activity, disrupts microtubules, modulates STAT1 signaling, reduces VEGF secretion, and induces a distinct cytokine profile, while synergizing with ruxolitinib, supporting its further preclinical development as a potential therapeutic strategy in myeloproliferative neoplasms.

Keywords: MPNs, STK405759, tubulin, microtubule targeting agent, JAK-STAT1 signaling, VEGF, ruxolitinib

Introduction

Myeloproliferative neoplasms (MPNs) are clonal hematologic diseases characterized by excessive proliferation of myeloid lineages in the bone marrow. MPNs are traditionally classified into Philadelphia-positive (BCR-ABL1) chronic myeloid leukemia (CML), which is characterized by increased granulocytic proliferation, and Philadelphia-negative MPNs, which include polycythemia vera (PV), marked by an increase in erythrocytes; essential thrombocythemia (ET), characterized by excessive platelet production; and primary myelofibrosis (PMF), a disorder in which normal bone marrow is progres-

sively replaced by fibrous tissue. Approximately 8.35% of PV, 1.85 of ET and up to 15% of PMF cases progress to secondary acute myeloid leukemia (AML), primary as a result of clonal evolution and the acquisition of additional somatic mutations [1].

Hematopoietic clones in BCR-ABL1-negative MPNs often harbor mutually exclusive driver mutations in genes involved in the JAK/STAT signaling pathway, such as Janus kinase 2 (JAK2), calreticulin (CALR), or myeloproliferative leukemia virus oncogene (MPL). The JAK2 V617F mutation is the most common, occurring in over 95% of PV cases, 50-75% of ET cases,

and 40-75% of PMF cases. CALR mutations are found in 15-30% of ET and PMF cases, while MPL mutations are present in 4-8% of cases. Less than 10% of patients are "triple-negative", lacking these common mutations [2].

The prognosis for ET and PV is generally favorable, with median survival estimates of 33 years for younger PV patients and 24 years for ET patients [3]. Cytoreductive therapy, typically with hydroxyurea, is recommended for high-risk individuals. However, up to 15% of patients may exhibit resistance or an inadequate response to hydroxyurea, which is associated with a poorer prognosis [4].

PMF, the most severe form of MPN, presents a broad median survival range, from as low as two to over twenty years, depending on clinical and molecular factors [5]. Allogeneic hematopoietic stem cell transplantation remains the only potential curative therapy for PMF and CML but is limited to a small subset of eligible patients. For high-risk myelofibrosis and hydroxyurea-resistant or intolerant PV patients, the JAK1/JAK2 inhibitors, including the first in class ruxolitinib, and the more recently approved fedratinib, pacritinib, and momelotinib, are the standard of care. Although these agents alleviate symptoms, reduce pro-inflammatory cytokines, and decrease splenomegaly, they do not prevent disease progression [6, 7]. In CML, tyrosine kinase inhibitors are widely used, but the most primitive stem cells remain resistant to these therapies [8].

Moderate to marked megakaryocytic hyperplasia is a hallmark of all types of MPNs, driven by increased megakaryocyte proliferation and a progressively impaired apoptotic signaling. These dysregulated megakaryocytes contribute significantly to the development of bone marrow fibrosis [9]. During maturation, megakaryocytes undergo endomitosis, a specialized cell cycle in which DNA replication occurs without cytokinesis, leading to the formation of large, highly polyploid cells [10]. Microtubules, composed primarily of tubulin, are essential for mitotic spindle function during endomitosis and play a central role in megakaryocyte differentiation and cell cycle regulation [11]. Given this dependency, megakaryocytes may be particularly susceptible to agents that disrupt microtubule dynamics.

STK405759, a synthetic small molecule, has previously shown significant efficacy in myelo-

ma, where it induces cell cycle arrest and apoptosis by disrupting microtubule dynamics. Importantly, it exhibited high cytotoxic activity against myeloma cell lines while maintaining low toxicity toward peripheral blood mononuclear cells, ultimately reducing tumor burden and prolonging survival in xenograft myeloma models [12, 13]. Based on these encouraging findings, we hypothesized that STK405759 may exert similar effects in MPNs, where megakaryocytes play a critical role in disease pathogenesis.

To evaluate the potential of STK405759 in MPNs, we selected three representative cell lines reflecting key disease features: HEL (erythroid, JAK2V617F-mutated), SET-2 (megakaryoblastic, JAK2V617F-mutated and wild type), and MEG-01 (BCR-ABL1-positive, modeling CML). These models enabled us to assess the compound's impact on megakaryocyterelated processes such as proliferation, microtubule integrity and cytokine secretion.

Materials and methods

Cell culture

Human HEL (ATCC Cat# TIB-180) and MEG-01 (ATCC Cat# CRL-2021) cells were cultured in RPMI-1640 medium, while HS-5 cells (ATCC Cat# CRL-11882) were maintained in DMEM medium. Both media were supplemented with 10% fetal calf serum and a penicillin-streptomycin antibiotic mix (Biological Industries, Kibbutz Beit Haemek, Israel). SET-2 cells (DSMZ Cat# ACC-608) were grown in RPMI-1640 medium supplemented with 20% fetal calf serum and the same antibiotic mix (Biological Industries). All cell cultures were maintained in a humidified incubator at 37°C with 5% CO_a. Routine mycoplasma testing confirmed that the cells were free from contamination. Cell line authentication was conducted using short tandem repeat (STR) profiling at the Genomics Center, Technion, Israel.

Cell viability assessment

Cells were seeded in 384-well plates and treated with graded concentrations of STK405759 (Mcule Inc., Pala Alto, USA), for different time intervals. Cell viability was determined using the XTT Cell Proliferation Kit (Biological Industries), according to the manufacturer's instructions. For combination treatment analy-

ses, cells were exposed to various concentrations of STK405759 and ruxolitinib (Sigma-Aldrich, St. Louis, MO, USA), either as monotherapies or in combination, for 72 hours. Half-maximal inhibitory concentration (IC $_{50}$) and combination indices were calculated using CalcuSyn software (version 2), based on the Median-Effect method.

Immunofluorescence analysis of apoptosis

Cells were treated with graded concentrations of STK405759 for 72 h. Apoptosis was evaluated by dual staining with Annexin V and propidium iodide (BD Biosciences, San Jose, CA, USA). Image acquisition and quantitative analysis were performed using the Operetta CLS™ High-Content Analysis System (PerkinElmer, Waltham, MA, USA).

Cell-cycle analysis

JAK2V617F-positive cells were treated with graded concentrations of STK405759 for 48 hours or with a fixed concentration of 50 nM STK405759 for different time intervals. MEG-01 cells were treated with various concentrations of STK405759 for 24 and 48 hours. Following treatment, cells were fixed in 70% ethanol and stored at -20°C. The next day, cells were stained with propidium iodide (50 µg/mL) containing RNase-A (20 units/mL; Sigma-Aldrich) for 30 minutes at 37°C. DNA content was analyzed using a CytoFLEX flow cytometer (Beckman Coulter, Brea, CA, USA) and FlowJo software (BD Biosciences).

Tubulin polymerization assay

Cells were treated with STK405759 for 48 hours and lysed in microtubule-stabilizing buffer containing 20 mM Tris-HCI (pH 6.8), 0.14 M NaCl, 1 mM EGTA, 0.5% NP-40, 1 mM MgCl₂, 0.4 µg/mL paclitaxel, protease inhibitor mixture (Roche, Basel, Switzerland), protease inhibitor cocktail 1 and 3 (Sigma-Aldrich), and 1 mM phenylmethylsulfonyl fluoride. Lysates were centrifuged to separate soluble tubulin (supernatant) from polymerized tubulin (pellet). Both fractions were subjected to immunoblotting with antibodies against α-tubulin, acetylated α -tubulin, β -tubulin, and GAPDH (all from Sigma-Aldrich). Protein bands were quantified using ImageJ software (version 1.53t, National Institutes of Health, Bethesda, MD, USA).

Immunofluorescence staining

Cells were treated with STK405759 for 72 hours. Following treatment, cells were fixed in 4% paraformaldehyde for 15 minutes and permeabilized with 0.3% Triton X-100 in PBS for 5 minutes at 37°C. Non-specific binding was blocked by incubating cells with 3% bovine serum albumin in PBS for 1 hour at room temperature. Cells were then incubated overnight at 4°C with either an anti-β-tubulin Alexa Fluor® 488 conjugated antibody (Merck) or a STAT1 (C-136) Alexa Fluor® 488 conjugated antibody (Santa Cruz Biotechnology, Dallas, TX, USA). Nuclei were counterstained with Hoechst 33342 (1 µg/mL). Immunofluorescence images were acquired using an Olympus Fluoview FV3000 confocal microscope (Olympus, Tokyo, Japan) or Zeiss LSM780 Inverted Confocal Microscope (Carl Zeiss AG, Germany).

Protein array analysis

Protein analysis was assessed using the Human Apoptosis Antibody Array (Abcam, Abcam, Boston, MA, USA), the Cytokine Human Membrane Antibody Array (Abcam), and the Human JAK/STAT Pathway Phosphorylation Array (RayBiotech, Peachtree Corners, GA, USA), following the manufacturers' protocols. Cells were cultured alone or with human HS-5 stromal cells and treated with 100 nM STK-405759 for 48 hours: untreated cells served as controls. For apoptosis and JAK/STAT arrays, cell lysates were collected; for the cytokine array, conditioned media was harvested and stored at -70°C. Equal protein amounts (800 µg per sample) were applied to the antibody-coated membranes, followed by incubation with antibodies. Signals were visualized by enhanced chemiluminescence and quantified using ImageQuant TL software (Cytiva, Marlborough, MA, USA). Spot intensities were normalized to reference controls on each membrane and further normalized to untreated group for comparative analysis.

Statistical analysis

Data were analyzed using one-way ANOVA, followed by post hoc t-tests with Bonferroni correction for multiple comparisons. Results are presented as the mean ± standard deviation (SD) of at least two or three independent experiments, each performed with multiple technical

replicates. Statistical significance was set at P < 0.05.

Results

Cytotoxic effects of STK405759 and its synergistic interaction with ruxolitinib in JAK2V617Fpositive MPN cells

HEL and SET-2 cells were exposed to graded concentrations of STK405759 for 24, 48, and 72 hours and viability was measured by XTT assay. STK405759 reduced cell viability in a concentration- and time-dependent manner. In HEL cells, the IC $_{50}$ values decreased from 0.666 at 24 hours to 0.160 at 48 hours and 0.139 μ M at 72 hours; in SET-2 cells, the IC $_{50}$ values were 0.620, 0.214, and 0.115 μ M at the respective time points (**Figure 1A, 1B**).

Next, we evaluated the potential synergistic cytotoxic effects of STK405759 in combination with ruxolitinib on JAK2V617F-positive cells. The combination treatment resulted in markedly greater cytotoxicity than either compound alone, with combination indices of 0.253 to 0.534, consistent with strong synergy in both cell lines (**Figure 1C-F**).

STK405759 disrupts microtubule organization in HEL and SET-2 cell lines

To assess the anti-microtubule effects of STK405759, HEL and SET-2 cells were treated for 48 hours, and the expression of soluble and polymerized α and β tubulin isoforms was analyzed by Western blot. In HEL cells, STK405759 treatment led to a marked reduction in polymerized β -tubulin and, to a lesser extent, polymerized α -tubulin (**Figure 2A**). In SET-2 cells, polymerized α - and β -tubulin levels were both reduced to comparable levels (**Figure 2B**). Additionally, acetylated α tubulin, a marker of microtubule stability [14], was significantly reduced in both cell lines.

Confocal microscopy of β -tubulin staining confirmed these findings, revealing disruption of the microtubule network in STK405759-treated cells. Both HEL and SET-2 cells exhibited tubulin bundling and accumulation, along with depolymerization at the spindle poles. Microtubule breakdown was accompanied by the appearance of apoptotic bodies. Notably, SET-2 cells displayed elongated cytoplasmic protrusions following treatment (Figure 2C, 2D).

STK405759 induces G2/M arrest in HEL and SET-2 cells

Treatment with STK405759 for 24 hours induced G2/M phase arrest in both HEL and SET-2 cells. By 48 hours, an increase in polyploidization was observed in both cell lines. In parallel, a significant accumulation of cells in the sub-G0 phase, indicative of apoptotic cell death, was detected as early as 24 hours and became more pronounced with prolonged drug exposure (Figure 3A, 3B).

To evaluate whether polyploidization was associated with megakaryocyte differentiation, CD41 expression was assessed by flow cytometry. While CD41 levels remained unchanged in HEL cells (Figure 3C), STK405759 treatment led to reduced CD41 expression in SET-2 cells (Figure 3D), suggesting that the observed polyploidy is more likely results from mitotic disruption rather than megakaryocyte differentiation.

STK405759 modulates apoptosis and JAK/ STAT signaling in HEL and SET-2 cells

STK405759 decreased cell viability primarily through the induction of apoptosis, with necrosis observed at higher concentrations, as determined by Annexin V/propidium iodide staining (Figure 4A, 4B). To gain insights into the molecular mechanisms underlying STK405-759-induced apoptosis, we examined apoptosis-related protein expression using a human apoptosis antibody array. Untreated HEL and SET-2 cells displayed similar baseline profiles of pro- and anti-apoptotic proteins. In HEL cells, STK405759 treatment led to a twofold upregulation of the tumor suppressor p53 (P=0.0045) along with significant downregulation of anti-apoptotic BCL-2 (-35%, P=0.038), pro-caspase 8 (P=0.004), and pro-caspase 3 (P=0.008) (Figure 4C).

SET-2 cells exhibited a distinct apoptotic profile following treatment, including a fourfold increase in IGFBP6 (P=0.003), and 1.5 to 1.7-fold increase in BAD (P=0.007), IGFBP2 (P=0.021), IGFBP4 (P=0.029), and HSP60 (P=0.036). STK405759 also reduced by more than 40% the expression of the decoy receptor TRAILR4 (P=0.028), the X-linked inhibitor-of-apoptosis XIAP (P=0.001), and to a lesser extent the anti-apoptotic BCL-2 (P=0.002) and BCL-w (P=0.003) proteins (Figure 4D).

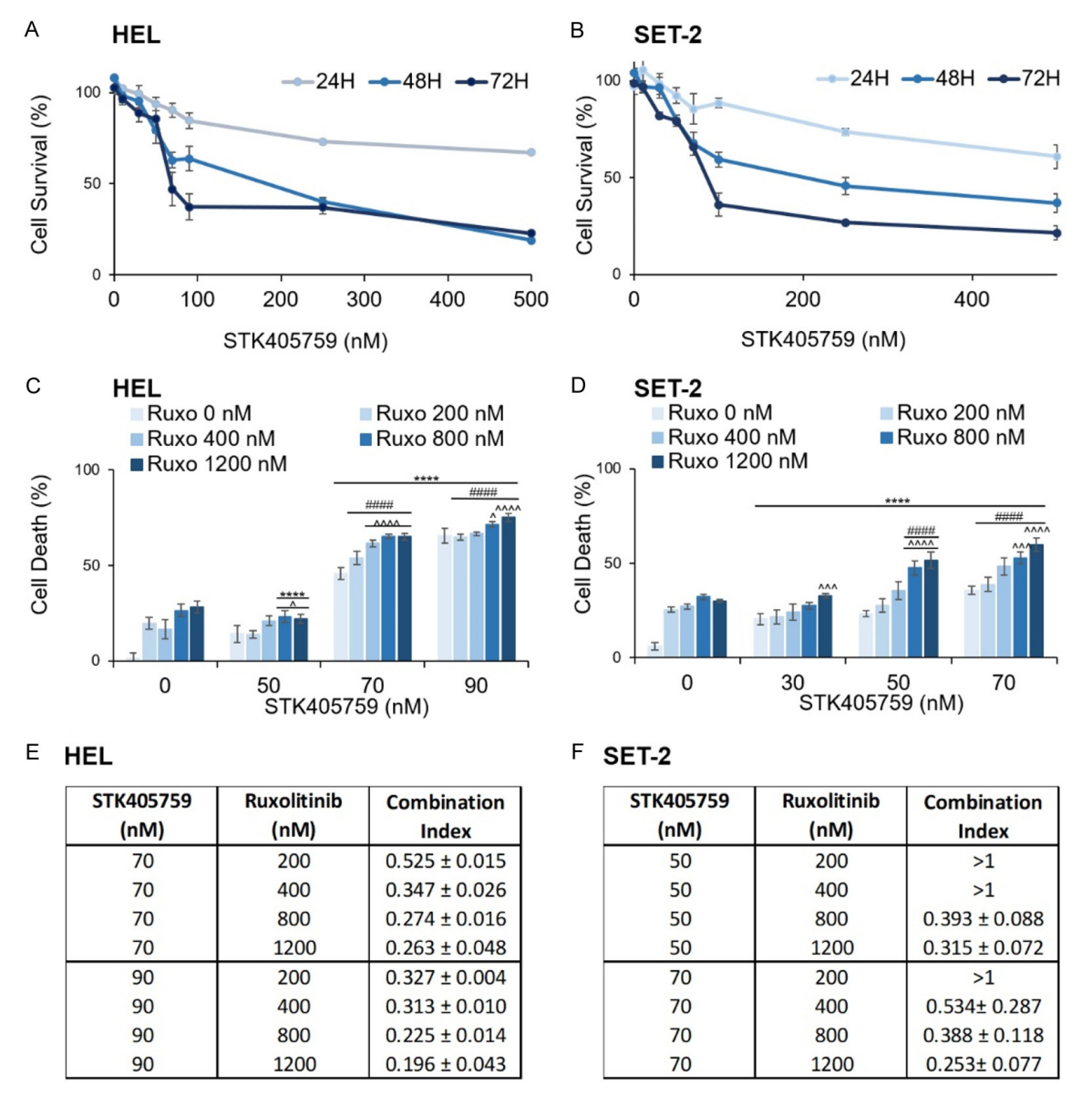


Figure 1. Cytotoxic effect of STK405759 on JAK2V617F-positive MPN cells. A, B. HEL and SET-2 cells were treated with graded concentrations of STK405759 for 24, 48, and 72 hours. Cytotoxicity was analyzed using the XTT assay. C, D. HEL and SET-2 cells were treated with STK405759, ruxolitinib or their combination at different concentrations for 72 hours. Cytotoxicity was analyzed by XTT assay. E, F. The combination index was calculated using CompuSyn software to evaluate drug interactions. All treatments were performed in triplicate across at least two independent experiments. Values were normalized to the drug-free control. Data are presented as mean \pm SE. ****P < 0.001 vs. control; ####P < 0.001 vs. ruxolitinib; ^^^P < 0.001, ^^P < 0.005 vs. STK405769.

Given the central role of the JAK/STAT pathway in MPN pathogenesis, we assessed the phosphorylation status of key pathways components following STK405759 treatment. STAT1 phosphorylation increased by 80% in SET-2 cells (P=0.004) and by 13% in HEL cells (P=0.006), while phosphorylation levels of JAK1, JAK2, STAT3, and STAT5 remained unchanged (Figure 5A, 5B).

Immunofluorescence analysis further demonstrated that STK405759 induced a dose-dependent retention of STAT1 in the cytoplasm and reduced its nuclear localization in both HEL and SET-2 cells, suggesting that the compound disrupts STAT signaling despite enhanced phosphorylation (Figure 5C, 5D). This effect was more pronounced in SET-2 cells.

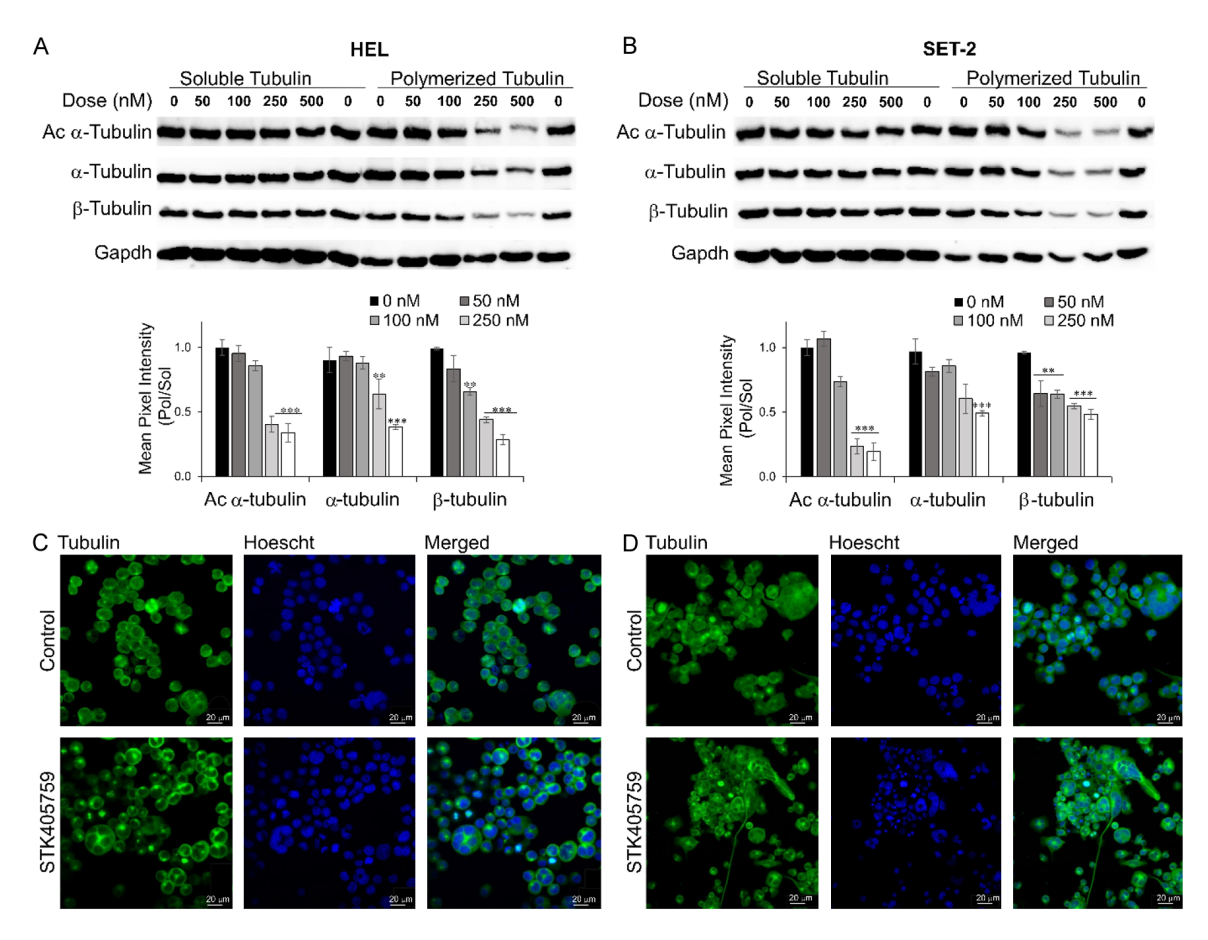


Figure 2. STK405759 disrupts tubulin dynamics on JAK2V617F-positive MPN cells. A, B. HEL and SET-2 cells were treated with graded concentrations of STK405759 for 48 hours. Polymerized (insoluble) and soluble tubulin fractions were separated and analyzed by immunoblotting to assess changes in tubulin dynamics. Data are presented as mean \pm SE. ***P < 0.005, **P < 0.01 vs. control. C, D. Cells were treated with 100 nM STK405759 for 48 hours, fixed and stained with an Alexa Fluor 488-conjugated anti-β-tubulin antibody (green) and Hoescht (blue) to visualize nuclei. Representative confocal images acquired using a Zeiss LSM780 Inverted Confocal Microscope illustrate disrupted microtubule organization. Scale bar: 20 μm. Magnification: 60×.

Effect of STK405759 on cytokine secretion in HEL and SET-2 cells

MPNs are characterized by chronic inflammation driven by both malignant and stromal cells, which reshape the bone marrow microenvironment to promote disease progression toward myelofibrosis [15]. Given the critical role of microtubules in cytokine secretion and their involvement in MPN pathogenesis, we examined whether STK405759 alters the cytokine secretory profile of HEL and SET-2 cells.

Under baseline conditions, both HEL and SET-2 cells secreted high levels of the pro-inflammatory cytokines GRO and IL-8, as well as the angiogenic factor VEGF. STK405759 treatment reduced VEGF secretion by more than 30% (P=0.0002) in HEL cells and by approximately

40% (P=0.0002) in SET-2 cells. In addition, SET-2 cells showed significant reductions in EGF (P=0.0025), and leptin (P=0.0011) levels following treatment (**Figure 6A, 6C**).

To explore the influence of bone marrow stromal cells on the response to STK405759, we co-cultured HEL or SET-2 cells with the human bone marrow stromal cell line HS-5. Compared to monocultures, co-cultures conditions led to increased secretion of inflammatory mediators including ENA-78, IL-6, GM-CSF, GRO- α , IL-1 α , IL-1 β , MCP-1 and MCP-3. STK405759 treatment significantly reduced VEGF secretion by 35% in HEL/HS-5 co-cultures (P=0.004) and by 66% in SET-2/HS-5 co-cultures (P=0.022). Additionally, STK405759 induced a two-fold increase in IL-1 β secretion in both co-culture models (**Figure 6B, 6D**).

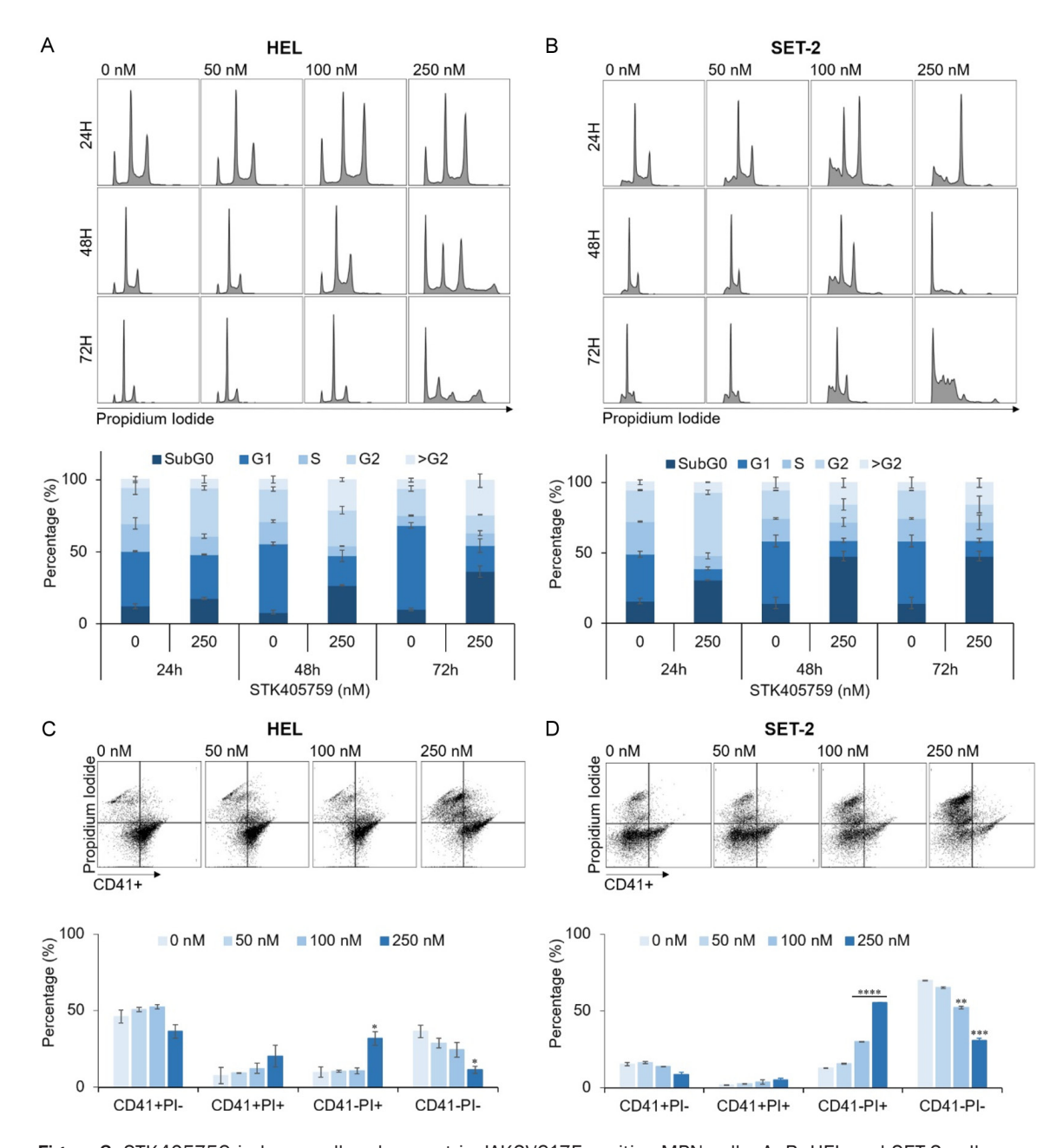


Figure 3. STK405759 induces cell cycle arrest in JAK2V617F-positive MPN cells. A, B. HEL and SET-2 cells were treated with graded concentrations of STK405759 for different time intervals. DNA content was detected by propidium iodide staining followed by flow cytometry analysis to evaluate cell cycle distribution. C, D. Flow cytometry plots (top) and corresponding quantification (bottom) of CD41 expression in HEL and SET-2 cells following treatment. All treatments were performed in at least two independent experiments. Values were normalized to the drug-free control. Data are presented as mean \pm SE. ****P< 0.001, **P< 0.005, **P< 0.05 vs. control.

For cytokines secreted at lower levels, STK405759 treatment led to a 30-50% reduction in the secretion of MCSF (P=0.002), RANTES (P=0.0001), SCF (P=0.045), SDF-1 (P=0.019), TARC (P=0.020), and ANG (P < 0.0005) in SET-2/HS-5 co-cultures (**Figure 6B**, **6D**). These findings indicate that STK405759 modulates a broad range of cytokine and

growth factors, suggesting that it may alter the inflammatory and fibrogenic milieu of the bone marrow in MPNs.

Cytotoxicity of STK405759 in philadelphia chromosome-positive MPN cells

To evaluate the anti-cancer potential of STK405759 in Philadelphia chromosome-posi-

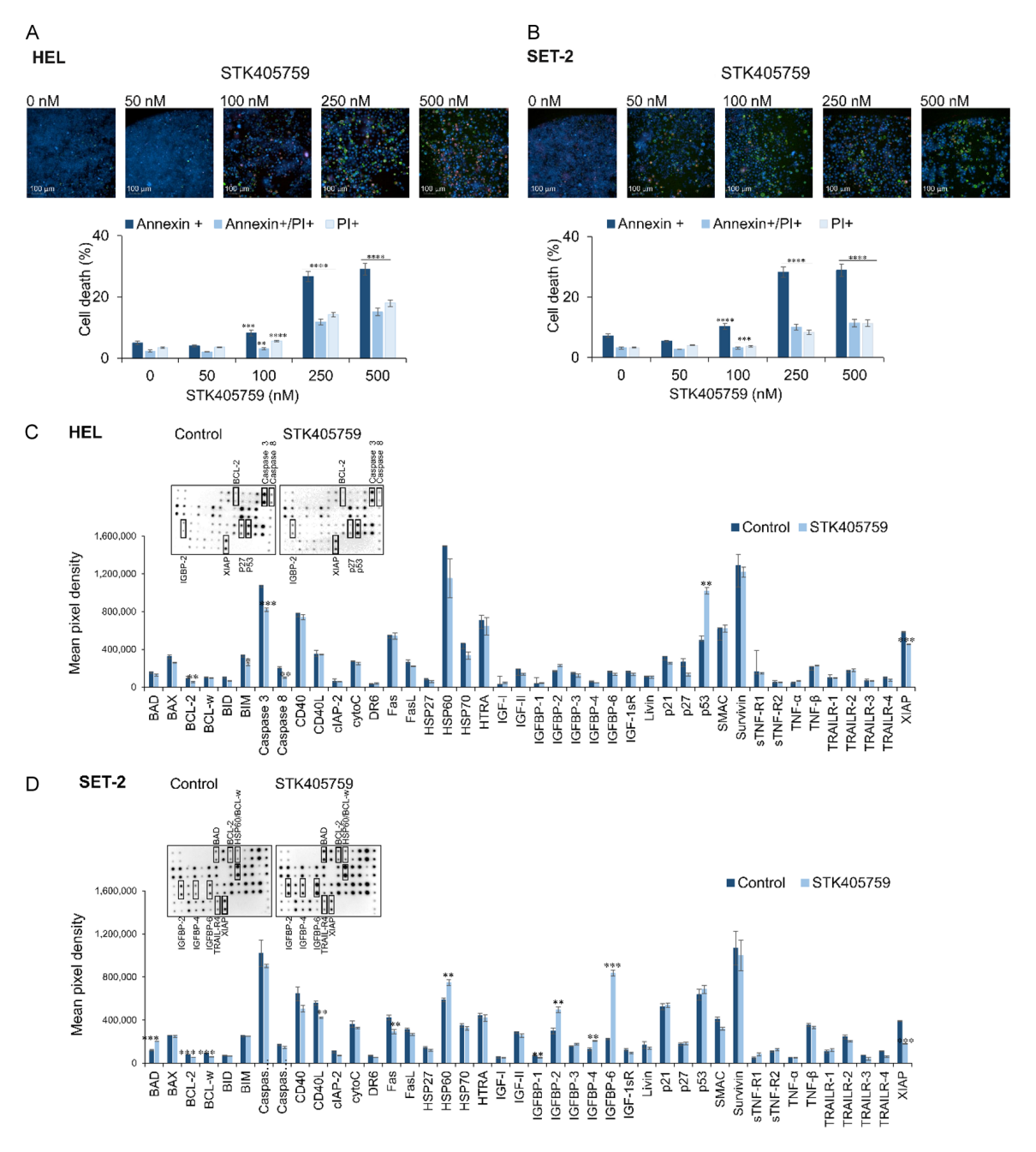


Figure 4. Apoptosis analysis of STK405759 treated JAK2V617F-positive MPN cells. (A, B) Apoptosis was evaluated by staining the cells with Annexin V (green) and propidium iodide (red) after STK405759 treatment for 72 hours, images were acquired using Operetta CLS^{TM} high-content analysis system and quantified with Harmony 4.5 software. Total cell death = Annexin V + propidium iodide positive cells. (C, D) HEL and (B) SET-2 cells were treated with 100 nM STK405759 for 48 h and then equal amounts of cellular proteins were subjected to a protein array using the Human Apoptosis Antibody Array Membrane. Spot intensities were normalized to reference array spots and then to untreated control. Data are presented as mean \pm SE. ****P< 0.001, ***P< 0.005, **P< 0.01 vs. control.

tive MPNs, we tested it effects on MEG-01 cells, a human megakaryoblast cell line derived from a patient with blast crisis CML. STK405759 significantly reduced MEG-01 cell viability in a concentration- and time-depen-

dent manner, with IC $_{50}$ values of 0.756 μ M, 0.123 μ M, and 0.125 μ M at 24, 48, and 72 hours, respectively. The observed cytotoxicity was associated with the induction of both apoptosis and necrosis (**Figure 7A, 7B**).

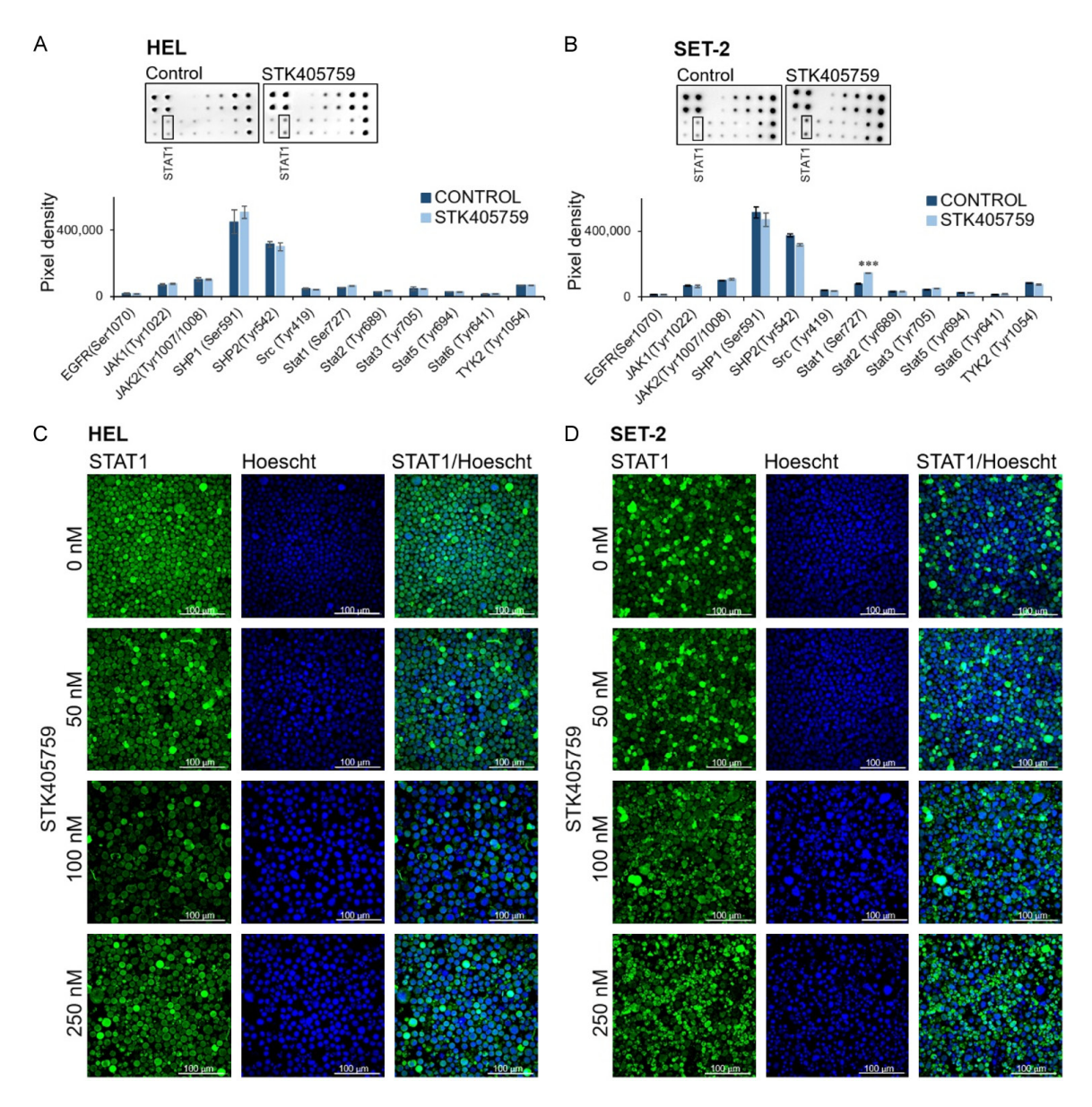


Figure 5. STAT1 signaling following STK405759 treatment in JAK2V617F-positive MPN cells. A, B. HEL and SET-2 cells were treated with 100 nM STK405759 for 48 hours. Equal amounts of cellular protein lysates were analyzed using the Human JAK/STAT Pathway Phosphorylation Array Membrane. Representative scanned images are shown. Spot intensities were normalized to reference array spots and then to untreated control. Data are presented as mean \pm SE. ***P < 0.005 vs. control. C, D. Representative immunofluorescence images depicting STAT1 expression and subcellular localization in HEL and SET-2 cells treated with increasing concentrations of STK405759. Nuclei were counterstained with Hoescht. Images were acquired using an Olympus Fluoview FV3000 confocal microscope. Scale bar: 100 µm. Magnification: 40×.

STK405759 treatment induced $\rm G_2/M$ phase arrest at 24 hours, followed by a marked increase in the sub- $\rm G_0$ population at 48 and 72 hours, indicating progressive cell death. Additionally, polyploidization became evident at later time points (**Figure 7C**). Consistent with its mechanism as a microtubule targeting agent (MTA), STK405759 induced a dose-dependent

decrease in α - and β -tubulin polymerization and disrupted mitotic spindle formation during cell division (**Figure 7D**, **7E**).

Importantly, STK405759 did not alter CD41 expression or STAT1 localization in MEG-01 cells, suggesting that its cytotoxic effects occur independent of megakaryocytic differentiation

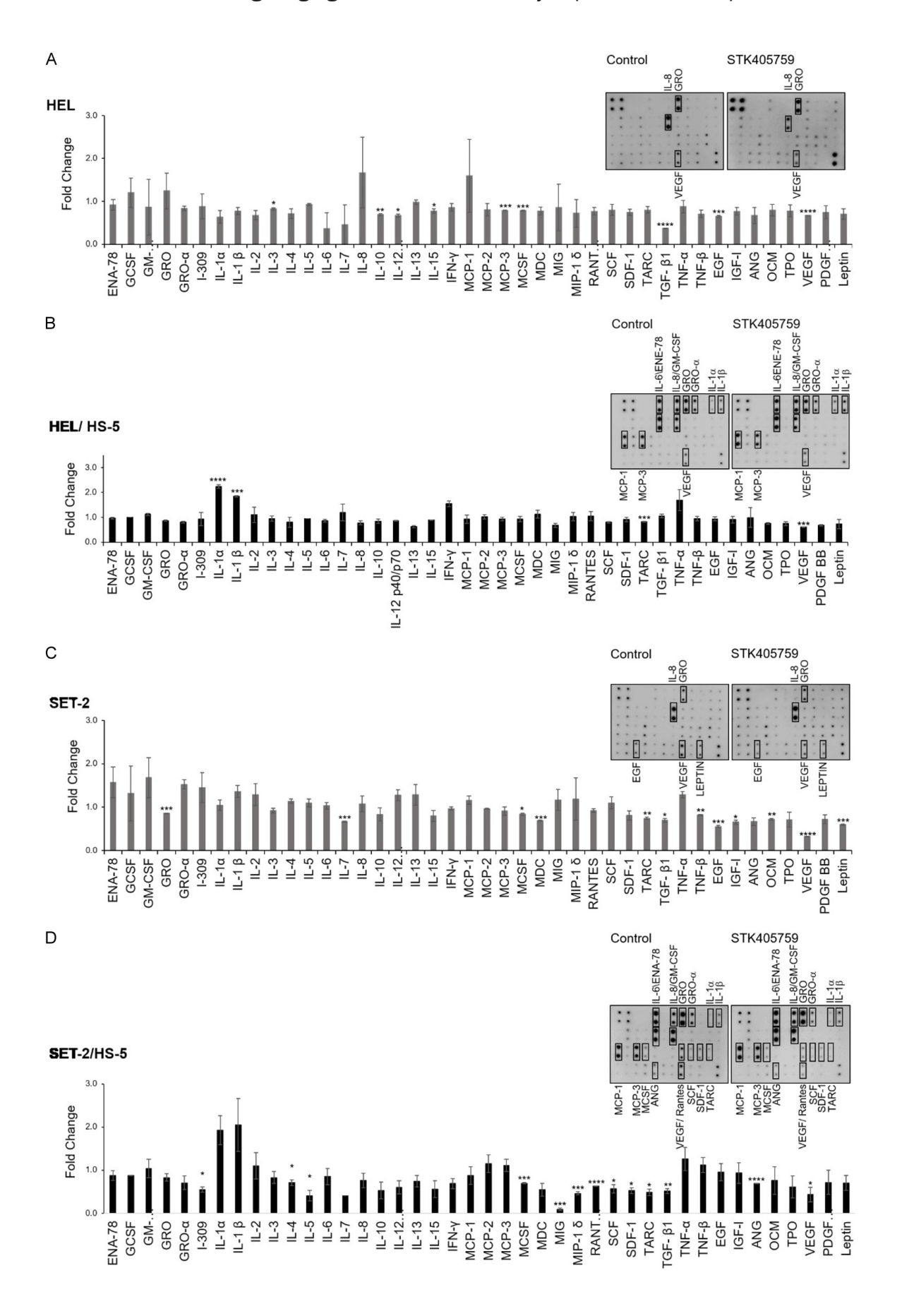


Figure 6. Cytokine protein array analysis of JAK2V617F-positive MPN cells treated with STK405759. (A, C) HEL and SET-2 cells cultured alone, and (B, D) co-cultured with HS-5 stromal cells were treated with 100 nM STK405759 for 48 hours. Equal amounts of secreted proteins were then analyzed using the Cytokine Human Membrane Antibody Array. Representative scanned images are shown. Spot intensities were normalized to reference array spots and then to untreated control. Data represent mean \pm SE from three independent experiments. ****P < 0.001, **P < 0.005 vs. control.

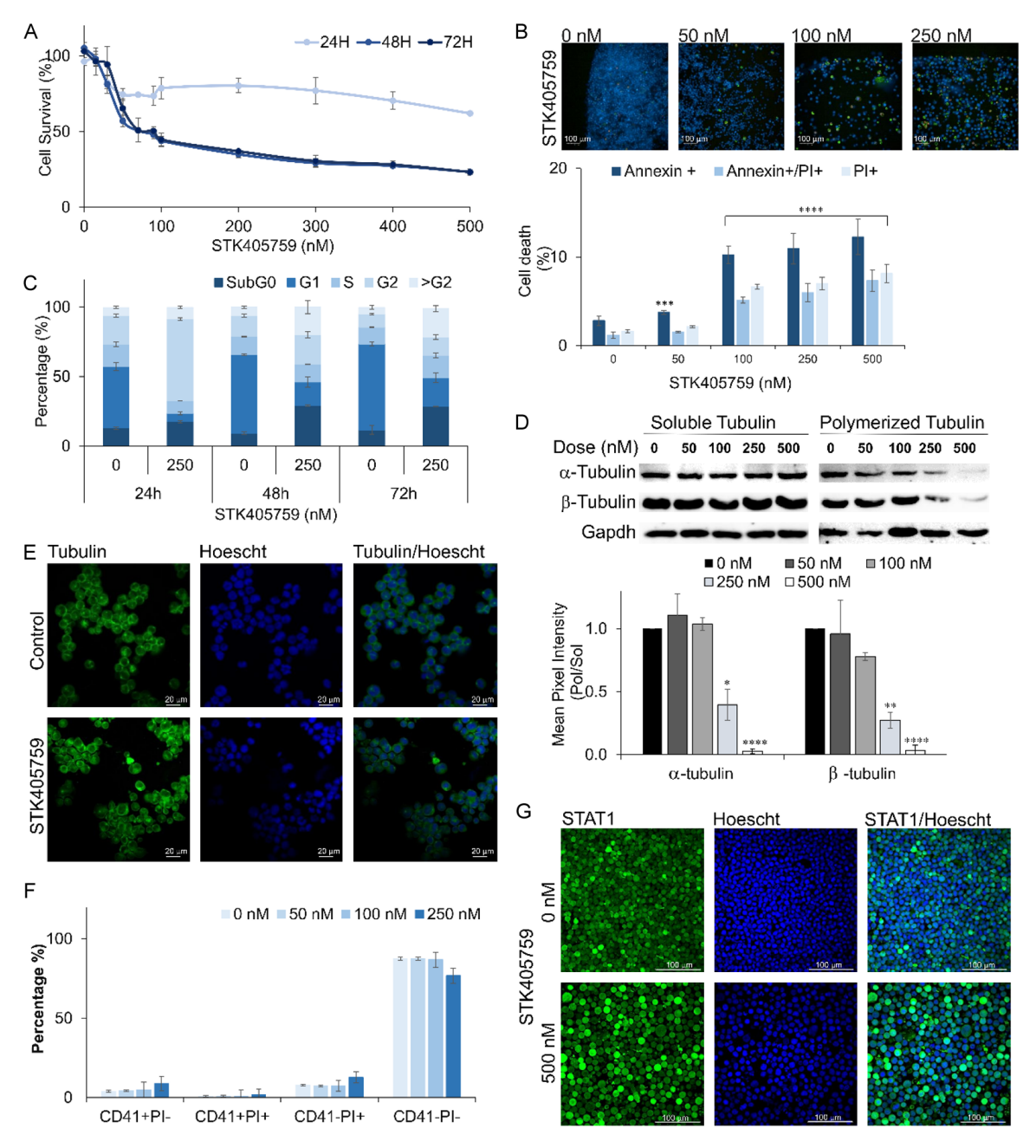


Figure 7. STK405759 cytotoxicity and mechanistic effects in BCR-ABL1-positive MEG-01 cells. A. Dose- and time-dependent cytotoxicity after STK405759 treatment measured by XTT assay, values expressed as % viability relative to control. B. Representative images of apoptosis detected by Annexin V (green) and propidium iodide (red) staining after treatment for 72 hours, images acquired using Operetta CLS™ and quantified with Harmony 4.5 software. Total cell death = Annexin V + propidium iodide positive cells. C. Cell cycle distribution following STK405759 treatment, analyzed by propidium iodide and flow cytometry. D. Polymerized and soluble tubulin fractions analyzed by immunoblotting. E. Representative confocal images of β-tubulin (green) and nuclei (Hoescht, blue) after 48 hours of treatment; captured using Zeiss LSM780 confocal microscope. F. CD41 expression levels following treatment. Scale bar: 20 μm. Magnification: 60×. G. Representative immunofluorescence images showing STA11 (green) expression

and subcellular localization after STK405759 exposure; nuclei counterstained with Hoescht (blue). Scale bar: 100 μ m. Magnification: 40×. Data represent mean \pm SE. ****P< 0.001, ***P< 0.005, **P< 0.01 vs. control.

pathways and STAT1 mediated signaling (**Figure 7F. 7G**).

Discussion

In this study, we showed that STK405759 exhibits potent cytotoxic activity in both BCR-ABL1-negative (HEL and SET-2) and BCR-ABL1-positive (MEG-01) MPN cell lines. STK405759 treatment induced concentration- and time-dependent $G_{\rm 2}/M$ phase cell cycle arrest, polyploidization, and both apoptotic and necrotic cell death. These effects were associated with disrupted α and β tubulin polymerization and impaired mitotic spindle assembly, consistent with its mechanism as a microtubule destabilizer agent. Additionally, STK40575 impacts MPN cells by modulating STAT1 signaling and reducing VEGF secretion.

Increasing evidence supports the therapeutic relevance of targeting cell cycle regulators in hyperproliferative hematopoietic progenitors. In this context, the CDK4/6 inhibitor palbociclib blocks G1/S transition in JAK2V617F-positive cells, reduces colony formation and synergizes with JAK inhibition [16]. Likewise, alisertib, a clinically tested Aurora kinase inhibitor, specifically targets dysregulated megakaryocytes, promoting their maturation and polyploidization while reducing bone marrow fibrosis, thereby highlighting the vulnerability of MPN cells at multiple cell cycle checkpoints [17]. In contrast, STK405759 acts through a distinct mechanism, directly destabilizing microtubules to induce growth arrest while simultaneously modulating STAT1 signaling, cytokine secretion, and angiogenesis. Together, these approaches converge on the megakaryocytic hyperplasia central to MPN pathogenesis, underscoring cell cycle disruption as a key therapeutic vulnerability and offering potential combinatorial opportunities or alternative strategies for different patient populations.

MPN cells harboring the JAK2V617F mutation exhibit increased JAK2 activity and elevated levels of phosphorylated STAT1 [18]. STAT1 is a key transcription factor that regulates apoptosis, differentiation, and immune activation, while also suppressing angiogenic factors such

as VEGF [19]. It signaling plays a central role in current therapeutic strategies, such as IFN-α therapy, which activates STAT1 signaling and preferentially targets disease-initiated stem cells through JAK1-STAT1-ROS activation [20]. Notably, STAT1 phosphorylation is elevated in JAK2V617F-positive ET patient derived cells [21], and in mouse MPN models. Conversely, STAT1 deficiency in the genetic context of JAK2-V617F promotes erythropoiesis while suppressing megakaryopoiesis [22], highlighting STAT1's critical role in lineage regulation. STK405759 markedly enhanced STAT1 phosphorylation and decreased its nuclear translocation in SET-2 cells, while producing only modest effects in HEL cells. STAT1 localization was unaffected in MEG-01 cells. These STAT1related differences correlated with sensitivity to STK405759, as cells showing pronounced effects on both tubulin dynamics and STAT1 activity showed lower IC50 values, likely because STK405759's microtubule-destabilizing effects, since intact microtubules are required for STAT1 nuclear import [23]. Importantly, the downstream consequences of microtubule disruption, including modulation of CD41 and STAT1 signaling, appeared more pronounced in cells with a JAK2-mutated/STAT1dependent signaling background, whereas BCR-ABL1-driven cells were less sensitive to these effects. This differential response highlights the context-dependent specificity of STK405759 for the JAK2/STAT axis in myeloproliferative neoplasm models. Further studies are warranted to evaluate STAT1 downstream transcriptional targets and to determine the functional consequences of impaired nuclear localization on gene expression in MPN cells. Collectively, these results suggest that STK405759 not only disrupts microtubule dynamics but also modulates key signaling pathways relevant to MPN pathogenesis, offering insights for potential combination strategies with JAK inhibitors.

Bone marrow from patients with PV, myelofibrosis and CML have been shown to exhibit increased vascularity [24], and elevated VEGF levels have been linked to JAK2V617F mutational status and disease severity [25]. STK405759 significantly decreased the secre-

tion of the pro-angiogenic factor VEGF in both HEL and SET-2 cells, including in co-culture with bone marrow stromal cells. Given the known roles of angiogenesis and stromal cell signaling in MPN progression, these findings highlight the dual effect of STK405759 on both malignant cells and their supportive niche.

Interestingly, STK405759 decreased tubulin acetylation yet paradoxically increased IL-1 β secretion in co-cultures of HEL and SET-2 with HS-5 stromal cells [26]. These findings contrast with previous reports in ATP activated macrophages, where microtubule-stabilizing agents such as paclitaxel enhanced IL-1 β release and increased tubulin acetylation, while destabilizing agents like nocodazole reduced acetylation and impaired IL-1 β secretion [26, 27]. Together, these results suggest that STK40-5759 induces a distinct inflammatory signature, warranting further investigation into the role of IL-1 β mediating its anti-tumor effects.

Previous studies have shown that paclitaxel mediated microtubule stabilization enhances ruxolitinib efficacy via STAT1 activation in JAK2V617F positive cells [28]. In contrast, our findings demonstrated that STK405759, a microtubule destabilizing agent, also synergized with ruxolitinib. This suggests that modulation of tubulin dynamics, whether through stabilization or destabilization, can potentiate JAK inhibition and may represent a promising combinatorial strategy in MPN therapy. The synergy between STK405759 and ruxolitinib, by simultaneously targeting JAK-STAT signaling and microtubule integrity, could provide meaningful clinical benefits. In ruxolitinib-refractory myelofibrosis, dual targeting could help overcome resistance, paralleling strategies already employed with second generation JAK inhibitors and other agents [29, 30]. In hydroxyurearesistant or intolerant PV and ET [31], particularly in patients with a JAK2V617F-positive background, this approach may enhance cytoreductive efficacy and mitigate megakaryocytic hyperplasia. Moreover, patients with massive splenomegaly, high fibrosis risk, or at risk of leukemic transformation, conditions in which aberrant angiogenesis is a key driver [32], may particularly benefit from STK405759's antiangiogenic effects, as current JAK inhibitor monotherapy remains largely symptomatic and fails to halt disease progression. This therapeutic rationale aligns with emerging combination strategies in MPNs, including ruxolitinib-based regimens, and parallels approaches using aurora kinase inhibitors in ruxolitinib-experienced patients [17, 33]. Further studies are warranted to better understand the mechanistic basis and clinical relevance of this synergy, particularly in populations with unmet therapeutic needs.

Recent findings highlight the therapeutic potential of tubulin binding agents in the treatment of AML. Microtubule disrupting antiparasitic drugs, such as mebendazole, have been repurposed as differentiation therapies in AML, showing promising preclinical activity [34]. More recently, a novel class of tubulin binding compounds including OXS0074172 and OXS0074643 was shown to induce G2/M cell cycle arrest and promote differentiation in AML cells, leading to reduced tumor burden in in vivo AML models [35]. While classical MTAs in clinical use, such as paclitaxel from Taxus brevifolia and vincristine from Catharanthus roseus, have shown anticancer activity in hematologic malignancies [36], STK405759 offers several advantages as a fully synthetic small molecule with superior manufacturing consistency, cost-effectiveness, and optimization potential. Its favorable selectivity profile was established in our previous work, where STK405759 exhibited potent cytotoxicity against myeloma cells while maintaining markedly lower toxicity toward peripheral blood mononuclear cells, together with the ability to overcome resistance relative to other MTAs [12, 13]. In the present study, we further demonstrate that STK405759 exerts differential effects in MPN cell lines, based on their JAK2-STAT1 background, reduced VEGF secretion and synergizes with ruxolitinib, highlighting its ability to target both proliferative and signaling pathways relevant to MPN pathogenesis and representing a distinct advantage compared to classical MTAs.

Although immortalized cell lines (HEL, SET-2, MEG-01) are widely used as MPN models [17, 37, 38], they limit the translational relevance of our findings. Future studies should validate these results in primary MPN patient samples with diverse genetic backgrounds and *in vivo* models to confirm the clinical applicability of STK405759.

Taken together, these findings indicate that STK405759 disrupts microtubule integrity and

induces apoptosis in both Philadelphia chromosome-negative (HEL and SET-2) and Philadelphia chromosome-positive (MEG-01) MPN cells, while modulating STAT1 signaling, with particularly strong effects in JAK2-mutated, STAT-dependent contexts, highlighting differential specificity. Beyond these effects, STK-405759 affects key extracellular factors, reducing the pro-angiogenic VEGF closely associated with disease progression and inducing a distinct inflammatory cytokine signature, including IL-1β in stromal-co-cultures. This dual impact on angiogenesis and inflammation suggests that STK405759 engages both microtubule-dependent tumor intrinsic and stromalimmune pathways contributing to its antitumor activity. The observed synergy with ruxolitinib underscores a promising combination strategy to enhance efficacy and overcome resistance. Overall, these results support further validation of STK405759 in preclinical models and clinical trials to assess its safety and therapeutic potential in MPN patients.

Acknowledgements

We gratefully acknowledge the support provided by the Israel Society of Hematology and Transfusion Medicine, Tel Hashomer Hospital, the Institute for Personalized and Translational Medicine, Ariel University, and a generous donation from Harel Meir.

Disclosure of conflict of interest

The authors disclose the following: G. Rozic and M. Leiba report a patent for WO2015097691 A1 issued. No potential conflicts of interest were disclosed by the other authors.

Abbreviations

AML, Acute Myeloid Leukemia; CALR, Calreticulin; CML, Chronic Myeloid Leukemia; ET, Essential thrombocythemia; MPL, Myeloproliferative leukemia virus oncogene; MPN, Myeloproliferative neoplasms; MTAs, Microtubule Targeting Agents; PMF, Primary myelofibrosis; PV, Polycythemia vera.

Address correspondence to: Gabriela Rozic, Department of Molecular Biology, Institute for Personalized and Translational Medicine, Ariel University, Kiryat HaMada 3, Ariel 40700, Israel. Tel: +972-3-9143033; E-mail: gabrielarozic@gmail.com

References

- [1] Auerbach S, Puka B, Golla U and Chachoua I. Recent advances towards the understanding of secondary acute myeloid leukemia progression. Life (Basel) 2024; 14: 309.
- [2] Luque Paz D, Kralovics R and Skoda RC. Genetic basis and molecular profiling in myeloproliferative neoplasms. Blood 2023; 141: 1909-1921.
- [3] Tefferi A, Guglielmelli P, Larson DR, Finke C, Wassie EA, Pieri L, Gangat N, Fjerza R, Belachew AA, Lasho TL, Ketterling RP, Hanson CA, Rambaldi A, Finazzi G, Thiele J, Barbui T, Pardanani A and Vannucchi AM. Long-term survival and blast transformation in molecularly annotated essential thrombocythemia, polycythemia vera, and myelofibrosis. Blood 2014; 124: 2507-2513; quiz 2615.
- [4] Demuynck T, Verhoef G, Delforge M, Vandenberghe P and Devos T. Polycythemia vera and hydroxyurea resistance/intolerance: a monocentric retrospective analysis. Ann Hematol 2019; 98: 1421-1426.
- [5] Tefferi A. Primary myelofibrosis: 2019 update on diagnosis, risk-stratification and management. Am J Hematol 2018; 93: 1551-1560.
- [6] Tefferi A. Primary myelofibrosis: 2023 update on diagnosis, risk-stratification, and management. Am J Hematol 2023; 98: 801-821.
- [7] Loscocco GG and Guglielmelli P. Targeted therapies in myelofibrosis: present landscape, ongoing studies, and future perspectives. Am J Hematol 2025; 100 Suppl 4: 30-50.
- [8] Corbin AS, Agarwal A, Loriaux M, Cortes J, Deininger MW and Druker BJ. Human chronic myeloid leukemia stem cells are insensitive to imatinib despite inhibition of BCR-ABL activity. J Clin Invest 2011; 121: 396-409.
- [9] Melo-Cardenas J, Migliaccio AR and Crispino JD. The role of megakaryocytes in myelofibrosis. Hematol Oncol Clin North Am 2021; 35: 191-203.
- [10] Machlus KR and Italiano JE Jr. The incredible journey: from megakaryocyte development to platelet formation. J Cell Biol 2013; 201: 785-796.
- [11] Liu H and Welburn JPI. A circle of life: platelet and megakaryocyte cytoskeleton dynamics in health and disease. Open Biol 2024; 14: 240041.
- [12] Rozic G, Paukov L, Cohen Z, Shapira I, Duek A, Bejamini O, Avigdor A, Nagler A, Koman I and Leiba M. STK405759 as a combination therapy with bortezomib or dexamethasone, in in vitro and in vivo multiple myeloma models. Oncotarget 2018; 9: 31367-31379.
- [13] Rozic G, Paukov L, Jakubikova J, Ben-Shushan D, Duek A, Leiba A, Avigdor A, Nagler A and

- Leiba M. The novel compound STK405759 is a microtubule-targeting agent with potent and selective cytotoxicity against multiple myeloma in vitro and in vivo. Oncotarget 2016; 7: 62572-62584.
- [14] Nekooki-Machida Y and Hagiwara H. Role of tubulin acetylation in cellular functions and diseases. Med Mol Morphol 2020; 53: 191-197.
- [15] Desterke C, Martinaud C, Ruzehaji N and Le Bousse-Kerdiles MC. Inflammation as a keystone of bone marrow stroma alterations in primary myelofibrosis. Mediators Inflamm 2015; 2015: 415024.
- [16] Dutta A, Nath D, Yang Y, Le BT and Mohi G. CDK6 is a therapeutic target in myelofibrosis. Cancer Res 2021; 81: 4332-4345.
- [17] Wen QJ, Yang Q, Goldenson B, Malinge S, Lasho T, Schneider RK, Breyfogle LJ, Schultz R, Gilles L, Koppikar P, Abdel-Wahab O, Pardanani A, Stein B, Gurbuxani S, Mullally A, Levine RL, Tefferi A and Crispino JD. Targeting megakaryocytic-induced fibrosis in myeloproliferative neoplasms by AURKA inhibition. Nat Med 2015; 21: 1473-1480.
- [18] Czech J, Cordua S, Weinbergerova B, Baumeister J, Crepcia A, Han L, Maie T, Costa IG, Denecke B, Maurer A, Schubert C, Feldberg K, Gezer D, Brummendorf TH, Muller-Newen G, Mayer J, Racil Z, Kubesova B, Knudsen T, Sorensen AL, Holmstrom M, Kjaer L, Skov V, Larsen TS, Hasselbalch HC, Chatain N and Koschmieder S. JAK2V617F but not CALR mutations confer increased molecular responses to interferon-alpha via JAK1/STAT1 activation. Leukemia 2019; 33: 995-1010.
- [19] Battle TE, Lynch RA and Frank DA. Signal transducer and activator of transcription 1 activation in endothelial cells is a negative regulator of angiogenesis. Cancer Res 2006; 66: 3649-3657.
- [20] Austin RJ, Straube J, Bruedigam C, Pali G, Jacquelin S, Vu T, Green J, Grasel J, Lansink L, Cooper L, Lee SJ, Chen NT, Lee CW, Haque A, Heidel FH, D'Andrea R, Hill GR, Mullally A, Milsom MD, Bywater M and Lane SW. Distinct effects of ruxolitinib and interferon-alpha on murine JAK2V617F myeloproliferative neoplasm hematopoietic stem cell populations. Leukemia 2020; 34: 1075-1089.
- [21] Chen E, Beer PA, Godfrey AL, Ortmann CA, Li J, Costa-Pereira AP, Ingle CE, Dermitzakis ET, Campbell PJ and Green AR. Distinct clinical phenotypes associated with JAK2V617F reflect differential STAT1 signaling. Cancer Cell 2010; 18: 524-535.
- [22] Duek A, Lundberg P, Shimizu T, Grisouard J, Karow A, Kubovcakova L, Hao-Shen H, Dirnhofer S and Skoda RC. Loss of Stat1 decreases

- megakaryopoiesis and favors erythropoiesis in a JAK2-V617F-driven mouse model of MPNs. Blood 2014; 123: 3943-3950.
- [23] Ma X and Sayeski PP. Identification of tubulin as a substrate of Jak2 tyrosine kinase and its role in Jak2-dependent signaling. Biochemistry 2007; 46: 7153-7162.
- [24] Lundberg LG, Lerner R, Sundelin P, Rogers R, Folkman J and Palmblad J. Bone marrow in polycythemia vera, chronic myelocytic leukemia, and myelofibrosis has an increased vascularity. Am J Pathol 2000; 157: 15-19.
- [25] Medinger M, Skoda R, Gratwohl A, Theocharides A, Buser A, Heim D, Dirnhofer S, Tichelli A and Tzankov A. Angiogenesis and vascular endothelial growth factor-/receptor expression in myeloproliferative neoplasms: correlation with clinical parameters and JAK2-V617F mutational status. Br J Haematol 2009; 146: 150-157.
- [26] Carta S, Tassi S, Semino C, Fossati G, Mascagni P, Dinarello CA and Rubartelli A. Histone deacetylase inhibitors prevent exocytosis of interleukin-1beta-containing secretory lysosomes: role of microtubules. Blood 2006; 108: 1618-1626.
- [27] Zeng QZ, Yang F, Li CG, Xu LH, He XH, Mai FY, Zeng CY, Zhang CC, Zha QB and Ouyang DY. Paclitaxel enhances the innate immunity by promoting NLRP3 inflammasome activation in macrophages. Front Immunol 2019; 10: 72.
- [28] Machado-Neto JA, de Melo Campos P, Favaro P, Lazarini M, da Silva Santos Duarte A, Lorand-Metze I, Costa FF, Saad ST and Traina F. Stathmin 1 inhibition amplifies ruxolitinib-induced apoptosis in JAK2V617F cells. Oncotarget 2015; 6: 29573-29584.
- [29] Talpaz M, Gerds AT, Lyons R, Langmuir P, Hunter D, Lamothe B, Hou K and McMahon B. A phase 2 study of itacitinib alone or in combination with low-dose ruxolitinib in patients with myelofibrosis. Leuk Res 2025; 155: 107732.
- [30] Rampal RK, Grosicki S, Chraniuk D, Abruzzese E, Bose P, Gerds AT, Vannucchi AM, Palandri F, Lee SE, Gupta V, Lucchesi A, Oh ST, Kuykendall AT, Patriarca A, Alvarez-Larran A, Mesa R, Kiladjian JJ, Talpaz M, Scandura JM, Lavie D, Harris M, Kays SK, Li Q, Boxhammer R, Brown B, Jegg AM, Harrison CN and Mascarenhas J. Pelabresib plus ruxolitinib for JAK inhibitor-naive myelofibrosis: a randomized phase 3 trial. Nat Med 2025; 31: 1531-1538.
- [31] Kuykendall AT. Treatment of hydroxyurea-resistant/intolerant polycythemia vera: a discussion of best practices. Ann Hematol 2023; 102: 985-993.
- [32] Thomas K, Rao R, G V C, Rai S, Rao A R S and Basavaraju Vatsala K. Study of significance of bone marrow microvessel density in myelopro-

Microtubule targeting agent STK405759 in myeloproliferative neoplasms

- liferative neoplasms in correlation with CD34 blasts, mast cell count and fibrosis. F1000Res 2023; 12: 503.
- [33] Gangat N, Marinaccio C, Swords R, Watts JM, Gurbuxani S, Rademaker A, Fought AJ, Frankfurt O, Altman JK, Wen QJ, Farnoud N, Famulare CA, Patel A, Tapia R, Vallapureddy RR, Barath S, Graf A, Handlogten A, Zblewski D, Patnaik MM, Al-Kali A, Dinh YT, Englund Prahl K, Patel S, Nobrega JC, Tejera D, Thomassen A, Gao J, Ji P, Rampal RK, Giles FJ, Tefferi A, Stein B and Crispino JD. Aurora kinase A inhibition provides clinical benefit, normalizes megakaryocytes, and reduces bone marrow fibrosis in patients with myelofibrosis: a phase I trial. Clin Cancer Res 2019; 25: 4898-4906.
- [34] Matsuo H, Inagami A, Ito Y, Ito N, Iyoda S, Harata Y, Higashitani M, Shoji K, Tanaka M, Noura M, Mikami T, Kato I, Takita J, Nakahata T and Adachi S. Parbendazole as a promising drug for inducing differentiation of acute myeloid leukemia cells with various subtypes. Commun Biol 2024; 7: 123.

- [35] Jackson TR, Vuorinen A, Josa-Cullere L, Madden KS, Conole D, Cogswell TJ, Wilkinson IVL, Kettyle LM, Zhang D, O'Mahony A, Gracias D, McCall L, Westwood R, Terstappen GC, Davies SG, Tate EW, Wynne GM, Vyas P, Russell AJ and Milne TA. A tubulin binding molecule drives differentiation of acute myeloid leukemia cells. iScience 2022; 25: 104787.
- [36] Kaul R, Risinger AL and Mooberry SL. Microtubule-targeting drugs: more than antimitotics. J Nat Prod 2019; 82: 680-685.
- [37] Nakajima K, Suzuki M, Kawashima I, Koshiisi M, Kumagai T, Yamamoto T, Tanaka M and Kirito K. The chaperone protein GRP78 released from MPN cells increases the expression of lysyl oxidase in a human stromal cell line. Leuk Res 2023: 134: 107389.
- [38] Kawashima I and Kirito K. Metformin inhibits JAK2V617F activity in MPN cells by activating AMPK and PP2A complexes containing the B56alpha subunit. Exp Hematol 2016; 44: 1156-1165, e1154.